American Mineralogist, Volume 108, pages 543–551, 2023

Effects of thermal annealing on water content and $\delta^{18}O$ in zircon

Chuan-Mao Yang[1,2,3,†], Xiao-Ping Xia[1,2,3,*], Yu-Ya Gao[3,4], Xue Wang[5], Wan-Feng Zhang[1,3], Ze-Xian Cui[1,3], Ya-Nan Yang[1,3], Qing Yang[1,3], and Yi-Gang Xu[1,2,3]

[1]State Key Laboratory of Isotope Geochemistry and CAS Center for Excellence in Deep Earth Sciences, Guangzhou Institute of Geochemistry, Chinese Academy of Sciences, Guangzhou 510640, China
[2]College of Earth and Planetary Sciences, University of the Chinese Academy of Sciences, Beijing 100049, China
[3]Southern Marine Science and Engineering Guangdong Laboratory (Guangzhou), Guangzhou 511458, China
[4]National Institute of Metrology, Beijing 102200, China
[5]College of Earth Science and Engineering, Shandong University of Science and Technology, Qingdao 266590, China

Abstract

Primary water and oxygen isotope composition are important tools in tracing magma source and evolution. Metamictization of zircon due to U-Th radioactive decay may introduce external secondary water to the crystal, thereby masking the primary water and oxygen isotope signature. Recently, Raman-based screening has been established to select the low-degree metamict zircons. However, such an approach may not be appropriate for ancient samples, in which nearly all zircons are metamict. It was reported that thermal annealing can potentially heal crystals and retrieve primary water content and $\delta^{18}O$ information from metamict zircons, given the weaker hydrogen bond of secondary water than that of primary water. Heating experiments at temperatures of 200–1000 °C over a period of 2–10 h reveal that annealing can effectively recover primary water and oxygen isotopes from metamict zircons. Primary water in crystalline and metamict zircons remains intact when heated at <700 °C, while secondary water can be effectively expelled from metamict zircons when heated at 600 °C for >4 h, which represent the optimal annealing treatment condition. Hydrothermally altered zircon is an exception. It only yields the minimum estimate of its primary water contents at 600 °C over a period of >4 h, probably due to partial primary water loss during metamictization for hydrothermal zircons. Moreover, the proportion of low-$\delta^{18}O$ (<4.7‰) zircon grains that may be influenced by secondary water dropped from ~21% at <600 °C to ~9% when annealed at >700 °C. This study therefore provides the basis for applying zircon water and $\delta^{18}O$ proxies to geologically ancient samples.

Keywords: Metamict zircon, secondary water, primary water, oxygen isotopes, thermal annealing, diffusion

Introduction

Zircon water content and oxygen-hafnium isotope compositions have been widely used as geochemical proxies in constraining igneous processes (Kemp et al. 2007; Liebmann et al. 2021; Meng et al. 2021; Pidgeon et al. 2013, 2017; Valley et al. 1994; Xia et al. 2021; Xu et al. 2021; Yang et al. 2022; Yao et al. 2021). Although zircon is a nominally anhydrous mineral (NAM), it always contains a trace amount of water during its crystallization from magma (hereby termed primary water) (De Hoog et al. 2014; Liebmann et al. 2021; Meng et al. 2021; Wang et al. 2018; Xia et al. 2021; Yang et al. 2022; Yao et al. 2021). Water diffuses slowly in zircon (cf. many other NAMs such as garnet and olivine), indicating that zircon can better retain the primary water content (Ingrin and Zhang 2016; Zhang 2015). It has been reported that primary water in zircon has the potential to be a sensitive magma hygrometer (Xia et al. 2021). Oxygen isotope composition is a powerful tool to trace the source of magma (Valley et al. 1994). For example, Kemp et al. (2007) identified the crust-mantle mixing origin of I-type granites of eastern Australia from O-Hf isotopes. Acquiring the primary water and oxygen isotope composition of zircon can thus reveal melting mechanisms and magmatic processes.

Water in crystalline zircon is mainly in the form of OH that is introduced by the hydrogrossular substitution and is charge balanced with other cations, such as REEs (Aines and Rossman 1986; De Hoog et al. 2014; Hoskin and Schaltegger 2003; Nasdala et al. 2001a; Trail et al. 2011; Woodhead et al. 1991b; Zhang et al. 2010). However, the U-Th radioactive decay in zircon would cause lattice damage and metamictization (Chakoumakos et al. 1987; Nasdala et al. 1995, 2001b; Palenik et al. 2003; Woodhead et al. 1991a). Crystal lattice of metamict zircon is expanded and open to infiltration of external secondary water (Nasdala et al. 2001a; Pidgeon et al. 2013), thereby masking the primary water content. For example, the water content in metamict zircon can be up to 16.3 wt% (Aines and Rossman 1986). In metamict zircons, water is present in the form of hydrous mineral inclusions or fluid inclusions (Woodhead et al. 1991b). In addition, some neutral H_2O molecules may be present along cracks and grain boundaries (Woodhead et al. 1991b). Since the oxygen isotope composition of secondary water may be different from that of zircon, the measured $\delta^{18}O$ of metamict zircon could deviate significantly from its original signature (Gao et al. 2014; Liebmann et al. 2021; Wang et al. 2014; Yang et al. 2022). Moreover, zircon with high-radiation damage has a different matrix effect from that of crystalline zircon (Allen

* E-mail: xpxia@gig.ac.cn. Orcid 0000-0002-3203-039X
† Orcid 0000-0002-6735-8272

0003-004X/23/0003–543$05.00/DOI: https://doi.org/10.2138/am-2022-8444

and Campbell 2012; Gao et al. 2014; Pidgeon 2014; White and Ireland 2012), causing more difficulties in calibrating instrument mass fractionation (Allen and Campbell 2012; Gao et al. 2014; White and Ireland 2012).

Uneven distributions of U and Th in zircons result in different degrees of metamictization, occasionally forming metamict and non-metamict zones in a single zircon grain (Nasdala et al. 1996). The most intuitive way to avoid metamictization effect is to select non-metamict zircon grains, for instance, by using in situ Raman to determine the degree of metamictization (Ewing et al. 2003; Nasdala et al. 1995, 2001b, 2003; Palenik et al. 2003; Schmidt and Nasdala 2020; Yang et al. 2022). Crystalline zircons commonly have sharp peaks and strong characteristic vibration peaks of Si-O tetrahedrons, e.g., $\nu_3(SiO_4)$ (Nasdala et al. 1995, 2001b). Raman peaks of metamict grains are relatively smooth, with a decrease in peak intensity and a shift in $\nu_3(SiO_4)$ position to lower wavenumber (Nasdala et al. 1995, 2001b). Based on the full-width at half maximum (FWHM) and Raman shift of $\nu_3(SiO_4)$, Yang et al. (2022) developed a screening method for the moderately metamict zircon.

This screening method, however, may not be effective for geologically ancient (e.g., Archean-Proterozoic) samples, in which most zircons are strongly metamict. It is, therefore, important to establish an approach enabling the geochemical proxies of zircon water and $\delta^{18}O$ for ancient metamict zircons. One way is to thermally anneal zircon, because the O-H···O hydrogen bond of secondary water in metamict zircons is likely weaker than that in pristine grains (due to the larger unit-cell volume of metamict zircons) (Nasdala et al. 2001a). Compared with crystalline zircon, water in metamict zircon would be expelled at a lower temperature (Nasdala et al. 2001a). Meanwhile, the damaged metamict zircon lattice can be thermally annealed, and hence the matrix effect in Secondary Ion Mass Spectrometry (SIMS) isotope analysis is eliminated (Allen and Campbell 2012; Pidgeon 2014; Zhang et al. 2003).

Previous studies yielded different behaviors of water in zircon during annealing (Aines and Rossman 1986; Caruba et al. 1985; Nasdala et al. 2001a; Woodhead et al. 1991b). Thermogravimetric curves revealed that zircon, whether crystalline or metamict, begins to dehydrate at a temperature even as low as 50 °C (Caruba et al. 1985; Nasdala et al. 2001a), and the water is largely expelled when the zircon is heated to a temperature of ~600 °C. In contrast, infrared (IR) spectra of heat-treated zircon revealed that water content in moderately metamict zircon rarely drop at/below 530 °C (Nasdala et al. 2001a; Woodhead et al. 1991b). Clearly more thermal annealing experiments are needed to assess the optimal annealing conditions (including heating temperature and time duration) to minimize the metamictization effect on SIMS water content and oxygen isotope analyses. In this article, zircon samples with different degrees of metamictization were selected for the thermal annealing experiment, with the aims of investigating: (1) whether secondary water is present in metamict zircon and (2) under what heating conditions can the secondary water be expelled completely.

Sample descriptions

Zircon samples selected for the experiment are (1) crystalline Penglai zircon megacryst (Li et al. 2010); (2) Suzhou A-type granite zircons with varying degrees of metamictization (Sz2, partially metamict) (Gao et al. 2014; Yang et al. 2022); and (3) Archean TTG gneiss zircons that are nearly all metamict (THX13120, fully metamict) (Cui et al. 2022). Metamictization degrees of THX13120 are lower than that of zircons in Sz2, with the highest metamictization degrees (Cui et al. 2022; Gao et al. 2014; Yang et al. 2022). Penglai zircon megacrysts from early Pliocene alkaline basalt (Hainan Island, South China) are in-house standards for oxygen and hafnium isotope analyses (Li et al. 2010). They have homogeneous oxygen isotope composition with the recommended $\delta^{18}O$ value of 5.31 ± 0.10‰ (2SD) (Li et al. 2010). The Penglai zircon has low water content (20–200 ppm; Yang et al. 2022). The Penglai zircon megacrysts were crushed into ~100 μm fragments. The Sz2 zircon is from the Early Cretaceous A-type granites near Suzhou city (Jiangsu, South China) and contains varying U (33–13 433 ppm, commonly high-U) and Th (13–17 028 ppm) contents (Gao et al. 2014). The degree of zircon metamictization varies greatly from crystalline to highly metamict, as revealed by Raman spectroscopy (Gao et al. 2014; Yang et al. 2022). The oxygen isotope ($\delta^{18}O$ = 3.5–6.5‰) and water content (600 to >5000 ppm) of Sz2 zircon are variable (Gao et al. 2014; Yang et al. 2022). The low-$\delta^{18}O$ zircons are associated with high-water content, probably due to the larger amount of meteoric water in the crystalline zircon lattice (Gao et al. 2014; Yang et al. 2022). THX13120 zircon is from a TTG gneiss (U-Pb age: 2.19 Ga) in the Paleoproterozoic Taihua Group, North China Craton (Cui et al. 2022; Diwu et al. 2014). The zircon is highly metamict, and the water content varies from 700 to 2100 ppm (median 1458 ppm) (Cui et al. 2022). Most Sz2 and THX13120 zircon grains are >100 μm long (Fig. 1).

Analytical methods

Thermal annealing

Zircon grains or fragments from the three samples were randomly assigned into different zircon fractions, placed inside silica crucibles, and then heated for 2 h in a muffle furnace to 200, 300, 400, 500, 600, 700, 800, 900, and 1000 °C under one atmospheric pressure (1 atm). The experiment was conducted at the Guangzhou Institute of Geochemistry, Chinese Academy of Sciences (GIGCAS), with a thermocouple installed in the muffle furnace for temperature measurement (±3 °C fluctuation). The heating rate was 15 °C/min. After heating, the annealed zircon samples were cooled quickly (<10 min) to room temperature. To assess the effect of heating time duration, different zircon fractions were heated at 600 °C for 4, 6, 8, and 10 h. Consequently, a total of 39 thermally annealed zircon samples were obtained.

SIMS zircon water and oxygen isotope analyses

All samples and zircon standards were mounted on a glass slide with double-sided adhesive tapes. Zircon SA01 (6.2‰) or Qinghu (5.4‰) was used as the external standard for oxygen isotope calibration (Huang et al. 2019; Li et al. 2013). The samples were then encapsulated in a tin alloy mount and polished to expose the zircon interior (Zhang et al. 2018). The samples were observed with cathodoluminescence (CL) imaging and reflected-light petrography to select the analysis spots that were free of cracks or inclusions (Fig. 1).

The zircon oxygen isotope and water contents were measured simultaneously with a CAMECA IMS 1280-HR SIMS at the GIGCAS. The zircon water content was obtained from the relationship between water contents and measured $^{16}O^{1}H/^{16}O$ values of several in-house reference materials (ZG3, ZG6, ZG7, D16314-2, D15395-3, D15395-4, GJ-1, 91500) (Xia et al. 2019). The analytical uncertainty of water content is ~10% (Xia et al. 2019). The $^{18}O/^{16}O$ value was normalized to the Vienna Standard Mean Ocean Water (VSMOW), whose $^{18}O/^{16}O = 0.0020052$. Details of the method have been described by Xia et al. (2019). The analysis chamber was cooled by liquid nitrogen to maintain a high vacuum of ~1.9×10^{-9} mbar, in which the detection limit of water is ~10 ppm. The widths of the quadratic sputtered area and analytical area are 50 and 30 μm (15 μm spot size + 15 μm rastering), respectively. The ^{16}O and ^{18}O signals were configured with 500 μm

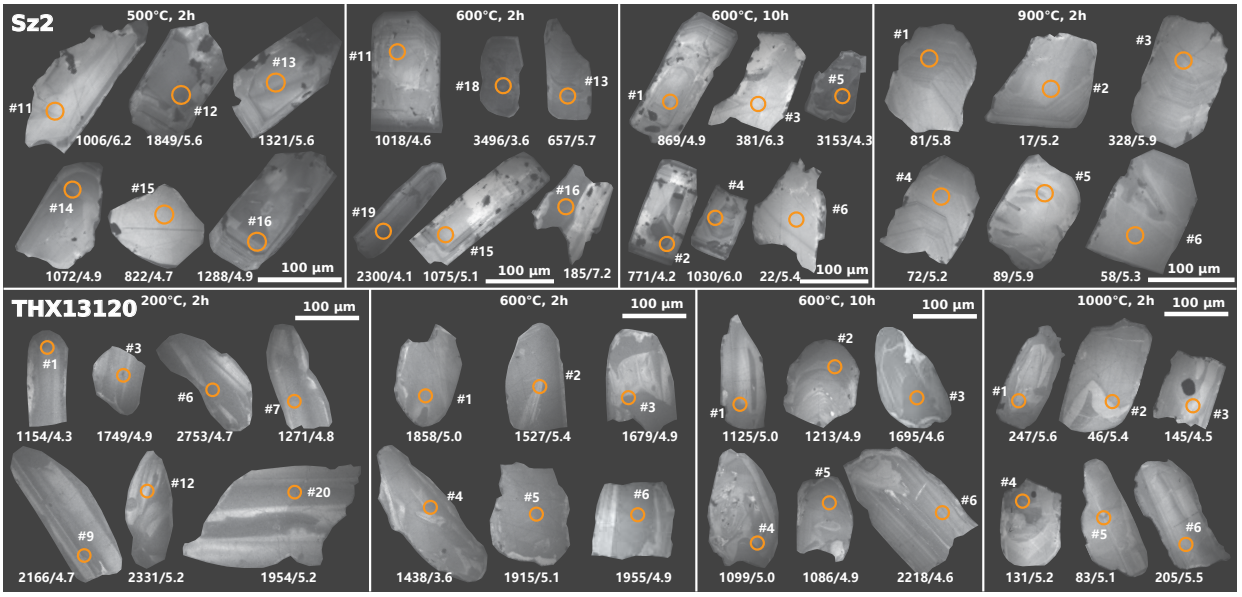

Figure 1. Cathodoluminescence images of Sz2 (upper) and THX13120 (lower) at different thermal annealing conditions. Orange circle represents SIMS analysis spots. The numbers below each zircon grains are water content (left) and $\delta^{18}O$ (right). Most zircon grains are >100 µm long.

collector slits to generate mass resolution power (MRP) of ~2500. To avoid ^{17}O interference, a 173 µm collection slit, corresponding to ~7000 MRP, was used for $^{16}O^{1}H$. The internal $^{18}O/^{16}O$ and $^{16}O^{1}H/^{16}O$ precisions are usually better than 0.4 and 0.5% (2SE), respectively.

Laser Raman spectroscopy

The analysis was performed with a Renishaw 2000 Raman spectrometer at the GIGCAS. The laser Raman spectral light source is a 532 nm argon laser. The telephoto objective lens has a 20× magnification, using 3 × 3 µm spot size. The Raman signal generated by a sample is split by a grating with 2400 grooves per millimeter, and then collected by a thermoelectrically cooled charge coupled device (CCD). The average spectral resolution is ~1 cm^{-1}. The time duration of spectral collection varies with the signal intensity (10–200 s). A full-wavelength spectrum of 100–1400 cm^{-1} was taken at one time, and a single-crystal silicon wafer was used to calibrate the Raman spectra before the measurement. The Raman shift of the single-crystal silicon wafer was corrected to 520.7 cm^{-1}. Note the Online Materials[1] Appendix Table S1 is available.

Results

Water contents and $\delta^{18}O$ values of zircons annealed at different temperatures

To evaluate the heating effect on pristine zircons, the Penglai zircon samples (20–200 ppm water) (Yang et al. 2022) were heated at <600, 700, 800, 900, and 1000 °C. As shown in Figure 2a, the zircon water content remains constant when heating at <700 °C, but drops to one third of its initial content at 700, 800, 900 °C, and rises slightly at 1000 °C (Fig. 2a). Water content of the untreated Sz2 zircon is relatively high (median 997 ppm) and variable (650 to >5000 ppm, mostly 750–2000 ppm) (Fig. 2b) (Yang et al. 2022). Significant water loss at ~700–800 °C is also observed (Fig. 2b). The median water content in zircons annealed at 600 °C is comparable to that of the untreated zircon. However, it is noteworthy that the water content below 400 °C rises with temperature and starts to fall when heated at >400 °C (Fig. 2b). The minimum water content at 500 °C (~460 ppm) is lower than that of the untreated zircon (~650 ppm). Slightly increasing water content at 1000 °C was also

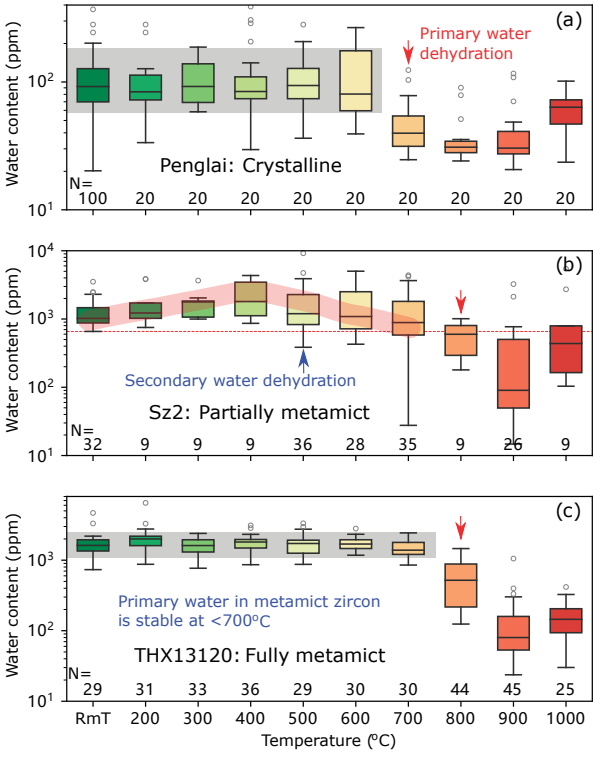

Figure 2. Water contents of zircons heated at different temperatures for 2 h. (**a**) Penglai: crystalline zircon. (**b**) Sz2: crystalline and coexisting highly metamict zircons. (**c**) THX13120: mostly metamict zircons. The Penglai and Sz2 zircon data at room temperature (RmT) are from Yang et al. (2022), and the THX13120 data (RmT) are from Cui et al. (2022). All the samples were placed inside a 50 °C oven before SIMS analysis to avoid surficial water adsorption from the air. The numbers of analysis spots are at the bottom of each panel.

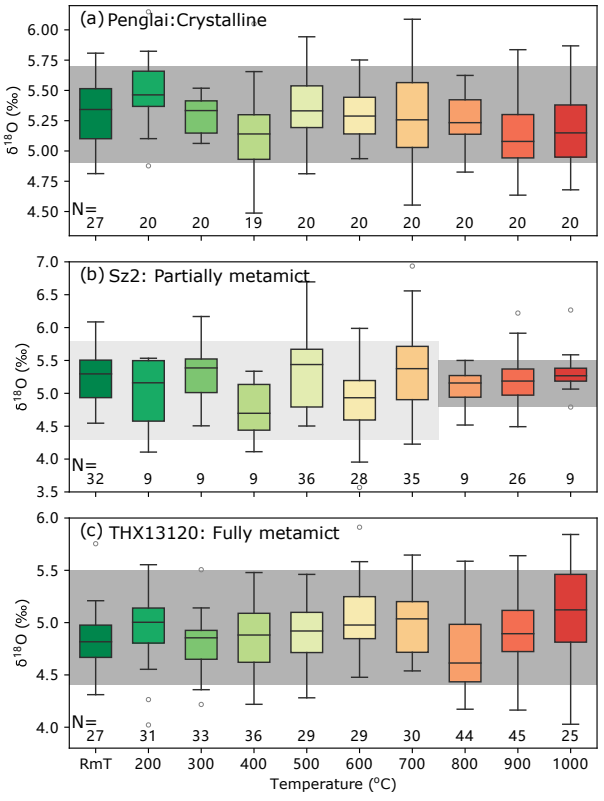

Figure 3. $\delta^{18}O$ variation for the zircon Penglai (**a**), Sz2 (**b**), and THX13120 (**c**) at different temperatures for 2 h. At >700 °C, the $\delta^{18}O$ variation for Sz2 becomes more limited.

observed (Fig. 2b). Water contents in the fully metamict THX13120 zircons annealed at 200–700 °C are similar (750–2000 ppm, median ~1500 ppm), and drop considerably to 505 ppm (median) when annealed at 800 °C. The water content is further reduced to 80 ppm (median) at 900 °C, approximately one-tenth of the untreated zircon water content (Fig. 2c).

Prominent oxygen isotope changes in zircon were only observed for Sz2 zircon samples (Fig. 3): the $\delta^{18}O$ range in zircons heated at >700 °C is much narrower than that heated <700 °C. Median $\delta^{18}O$ values for individual Penglai and TH13120 zircons heated at various temperatures are all consistent within error, even when a substantial amount of secondary water is expelled from zircons at >700 °C (Fig. 3).

Water contents and $\delta^{18}O$ values of zircons annealed at 600 °C for different time durations

For the Penglai and THX13120 zircons annealed at 600 °C, their water contents remain constant irrespective of the heating duration (Figs. 4a and 4c). The water content range and median value of Sz2 zircon remain relatively constant when the time duration is no more than 4 h (Fig. 4b). In contrast, the maximum, minimum and median water contents decrease, and the variation range becomes narrower when the zircons were heated for 6 h or longer (Fig. 4b). However, the oxygen isotopes of all the three zircon samples are virtually unaffected by the heating duration (Fig. 5).

Raman spectra of annealed zircons

The Penglai zircons always display intrinsic sharp Raman peaks when heated at 200–1000 °C, indicating no structural transformation of crystalline zircon. In contrast, Raman spectra of Sz2 zircon samples show both sharp and very flat Raman spectra for the untreated grains and those annealed at <400 °C (Fig. 6a). The Raman peaks became sharper when the temperature was increased to 800 and 1000 °C (Fig. 6a). All the unannealed THX13120 zircon grains are characterized by broad spectra and wide $\nu_3(SiO_4)$ (FWHM >8 cm^{-1}; Fig. 6b). Although there is a larger fraction of metamict zircons in THX13120 than in Sz2, the metamictization degree of THX13120 is generally lower than that of Sz2, as indicated by their smoother Raman spectra and $\nu_3(SiO_4)$ width (Fig. 6). Up to 600 °C, only few zircon grains exhibited crystalline zircon spectra, while most THX13120 zircon grains were transformed into crystalline at 1000 °C (Fig. 6b).

Discussion

Primary and secondary water in crystalline and metamict zircons

Secondary water is absent in Penglai zircons because these zircons are completely crystalline, and thus only primary water dehydration occurred during the annealing. As shown in Figure 2a, the diffusion loss of solely primary water started at 700 °C, and the water content fell to about half of that for the unannealed grains

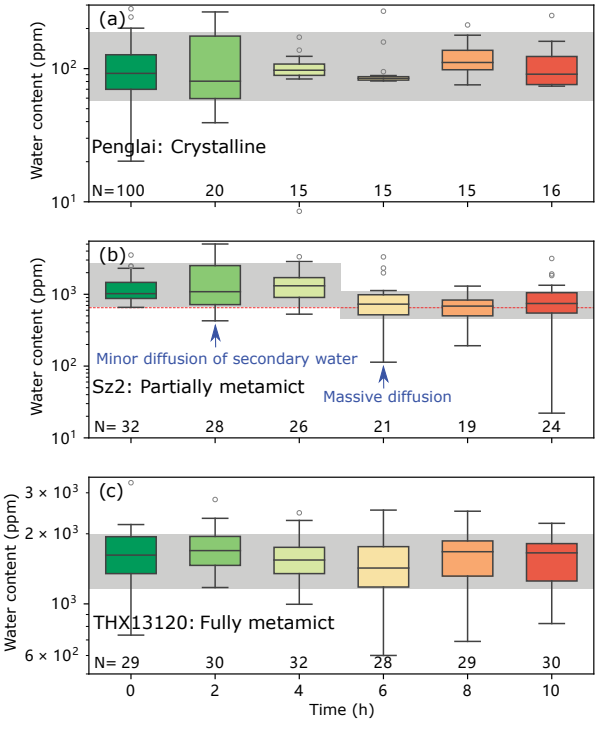

Figure 4. Water contents in three zircon samples: Penglai (**a**), Sz2 (**b**), and THX13120 (**c**), heated at 600 °C for different times. The data at room temperature are the same as in Figure 2. Note that the water contents of Penglai and THX13120 do not change with annealing time. There is minor secondary water diffusion in Sz2 annealed for <4 h, and massive diffusion when annealed for over 6 h.

(Fig. 2a). Primary water in the Penglai zircon samples remains constant at <700 °C. Although THX13120 zircon is strongly metamict and has more water, dehydration only occurred when it was heated at ~800 °C (Fig. 2c). The similar water behavior between the Penglai and THX13120 samples implies the presence of only primary water (i.e., no secondary water) in THX13120. This is because although metamictization can produce space for secondary water storage (Nasdala et al. 2001a), secondary water would not necessarily enter these spaces (Nasdala et al. 2001a; Yang et al. 2022). This is further supported by the phenomenon that secondary water dehydration was not observed during the annealing (Figs. 2 and 3). Thus, primary water in metamict zircon is as stable as in crystalline zircon, and some old, strongly metamict zircons can still retain their primary water content.

Previous studies have documented that the Taihua Group underwent upper amphibolite to granulite facies metamorphism with a peak metamorphic age of ~1.92 Ga (Lu et al. 2017; Zhai et al. 2005). Pseudosection modeling suggests metamorphic temperature may reach >800 °C (Lu et al. 2017). As a result, the primary water content may have been reset during metamorphism. However, TTG samples with similar compositions and metamorphic degrees but different tectonic settings in Taihua Group have distinct zircon water contents, implying primary water in zircon are not disturbed (Cui et al. 2022). This is either because metamorphic temperature is not as high as predicted by modeling or the onset temperature for primary water loss is higher at the metamorphic condition than that for our experiment

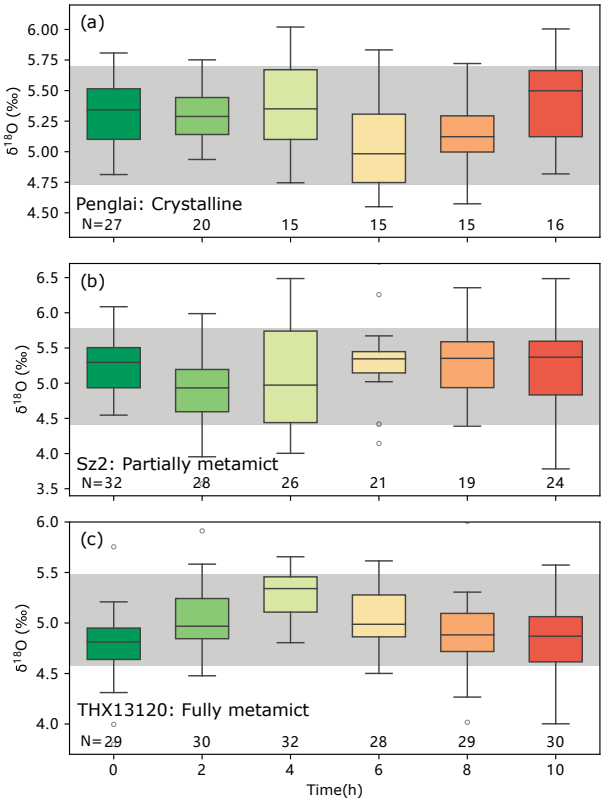

Figure 5. The $\delta^{18}O$ of three zircon samples annealed at 600 °C for different times: Penglai (**a**), Sz2 (**b**), and THX13120 (**c**).

due to the higher pressure.

As in Penglai and THX13120 zircons, intensive dehydration was observed in Sz2, which contains both metamict and crystalline zircons (Figs. 2 and 4) when heated at 700–800 °C, yet moderate dehydration also occurred in Sz2 at <600 °C (Fig. 2b). The Sz2 water content significantly dropped when heated at 600 °C for over 4 h (Fig. 4b). Probably, this may have resulted from the escape of secondary water, since primary water in both crystalline and metamict zircons are stable under such low temperatures. It is interesting that the onset temperature of primary water loss in the crystalline Penglai zircons (~700 °C) is lower than that of metamict THX13120 and Sz2 zircons (~800 °C) (Fig. 2). The temperature difference is attributed to a lower content of REE in Penglai zircon grains, which may weaken the chemical bonding of water. Furthermore, lower water contents in Penglai zircons make its loss at a lower temperature more noticeable (Cui et al. 2022; Yang et al. 2022).

Both secondary and primary water are present in Sz2, but only primary water is present in THX13120. This brings the question of whether (and if so, how) one can assess the presence of secondary water in a given sample. In Sz2, water and $\delta^{18}O$ contents are highly variable and high-water content is associated with low $\delta^{18}O$ (Fig. 7a) (Yang et al. 2022), suggesting a meteoric origin for the secondary water (Gao et al. 2014; Yang et al. 2022). In contrast, the water and $\delta^{18}O$ contents in THX13120 fall into a narrow range with no discernible correlation, again indicative of the lack of secondary water (Fig. 7b). Since water content in zircon is commonly <2000 ppm, the very high water content (e.g., >5000 ppm) in Sz2 thus suggests secondary water occurrence (Cui et al. 2022; Meng et al. 2021; Xia et al. 2019, 2021; Yang et al. 2022; Yao et al. 2021). Additionally, LREE-enrichment in some Sz2 zircon grains may also be hydrothermal alteration-related (Figs. 7c–7d). In contrast, magmatic zircons in THX13120 are all unaltered (Bell et al. 2016; Hoskin 2005). In short, markedly variable water and oxygen isotope contents with negative correlation and hydrothermal-type REE compositions, as well as flat Raman spectra could collectively be regarded as the diagnostics of presence of secondary-water in zircons.

The presence of appreciable amounts of water in zircons heated to >800 °C deserves explanation (Fig. 2). It was suggested that there may be more stable primary water in zircons (Caruba et al. 1985; Nasdala et al. 2001a; Zhang et al. 2010). When heated at >900 °C, all the three samples show a slight water content increase (Fig. 2), which can be attributed to the absorption of atmospheric water by zircon at 1000 °C or the uneven distribution of water in zircon.

Optimal annealing conditions to obtain reliable primary water content

To obtain reliable primary water content from metamict zircons, it is essential to formulate suitable annealing conditions to remove all secondary water while keeping primary water as much as possible. As discussed above, the primary water begins to escape at 700–800 °C, and the water content remains constant at <700 °C for both crystalline and metamict zircons. The critical temperature of ~700 °C for primary water diffusion is supported by IR analysis of previous stepwise heating experiments (Nasdala et al. 2001a; Woodhead et al. 1991b). Accordingly, a maximum

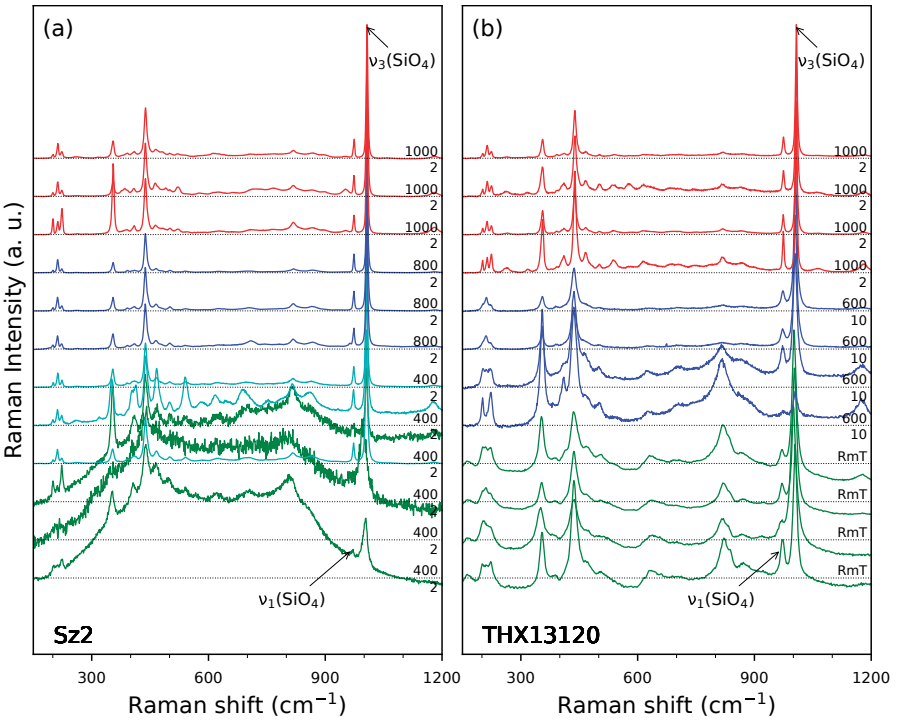

Figure 6. Comparison of Raman spectra of zircon Sz2 (**a**) and THX13120 (**b**) annealed at different temperatures. Labels on the right represents the annealing temperature (upper, °C) and time (lower, hour). The metamict zircon is distinct from crystalline zircon by its smooth spectrum. The spectra are displayed with different colors for clarity. Highly metamict zircons in Sz2 are still present when heated at 400 °C, but disappeared at 800 and 1000 °C. Most untreated zircons (at RmT) of THX13120 are metamict. Some metamict zircons are healed at 600 °C, and most become crystalline at 1000 °C.

annealing temperature of 600 °C was set to retrieve the primary water content (Fig. 4a).

Dehydration of primary water is also dependent on the zircon grain size and diffusion direction along the crystal axis (Ingrin and Zhang 2016; Zhang 2015). To investigate their effects, a series of modeling was conducted based on the hydrogen diffusion rate in zircon. Recent hydrogen-deuterium (H-D) exchange experiments yielded two different diffusion rates along three axes of zircon crystal (Ingrin and Zhang 2016; Zhang 2015). The diffusion rate along [001] is higher than those along [100] and [010] (Ingrin and Zhang 2016; Zhang 2015), which can be expressed as:

$$D_{[100][010]} = D_0 \exp\left[\frac{-(374 \pm 39)\,\text{kJ/mol}}{RT}\right],\ \log D_0(\text{m}^2\text{s}^{-1}) = 2.24 \pm 1.57$$

$$D_{[001]} = D_0 \exp\left[\frac{-(334 \pm 49)\,\text{kJ/mol}}{RT}\right],\ \log D_0(\text{m}^2\text{s}^{-1}) = 1.11 \pm 0.22$$

where D = diffusion coefficient; R and T = ideal gas constant and temperature, respectively.

In this study, the largest diffusion coefficient along the [001] direction was used. A one-dimensional diffusion equation was used to simulate the water behavior in zircon, assuming that the water content on the zircon grain margin is 0 ppm (Xu et al. 2019):

$$\frac{c}{c_0}(x,t) = \frac{4}{\pi}\sum_{j=0}^{\infty}\frac{1}{2j+1}\sin\frac{(2j+1)\pi x}{h}\cdot\exp\left(-\left[\frac{(2j+1)\pi}{h}\right]^2 Dt\right)$$

where c/c_0 is the ratio of the annealed zircon water content c to its initial water content c_0; h is the length of zircon grain in m; D is diffusion coefficient of zircon in m^2s^{-1}; t is diffusion time in s; and j is index of summation. The first 300 items on the right side of the equation were used in the calculation.

The fractions of preserved water at variable temperatures and positions in 100 μm zircon are illustrated in Figure 8. The water in zircon does not diffuse out until ~700 °C, and the diffusion occurs only on the zircon margins (<10 μm from margin) at 700–850 °C. At 900–1000 °C, zircon can preserve only 0–40% of the original water content, with the water in the core largely expelled (Fig. 8). The simulated fractions of preserved water at different temperatures are comparable with our thermal annealing experimental results (Fig. 2). Modeling with smaller zircon grains (40 μm long) for a longer duration of heating (6 and 10 h) shows that zircon water content remains stable at 600 °C, and a minor amount of water may be diffused out along the zircon margins at 700–800 °C.

Our modeling results suggest that secondary water starts to escape at <600 °C. Nevertheless, the median water content in Sz2 (heated at ~600 °C for 2h) is not lower than that of unannealed zircon (Fig. 2b), and the water content actually increases when heated at 200–400 °C (Fig. 2b). Such a phenomenon was also observed in IR spectrum from stepwise heating experiment, and has been attributed to the movement of hydrogen in a disordered site to an ordered site (Woodhead et al. 1991b). The water content in Sz2 begins to decrease from 400 to 600 °C (Fig. 2b), with the lowest water content (~250 ppm) occurring at 500 °C, even lower than that of unannealed zircons (~600 ppm; Fig. 2b) (Yang et al. 2022). This suggests that at 500 °C, secondary water is unstable and subject to mild diffusion loss. Therefore, heating of zircons at 600 °C for >4 h likely represents the optimal annealing conditions, which ensure the complete removal of secondary water and retain the maximum amount of primary water (Fig. 4b).

Retrieving primary water content and $\delta^{18}O$ by thermal annealing

It is noteworthy that the water content in Sz2 metamict zircons (annealed at 600 °C for >4 h) is lower than the primary water content estimated from crystalline zircons (screened by Raman spectra) (Fig. 9a) (Yang et al. 2022). This suggests that some primary water in Sz2 metamict zircon was lost either during the annealing or metamictization. Since primary water in both crystalline and metamict zircons is stable at <700 °C (Figs. 2 and 4), the primary water loss in Sz2 most likely resulted from geological processes rather than from thermal annealing. The Suzhou alkaline granites were variably hydrothermally altered, which may have affected the zircons and influenced the primary water content (Liebmann et al. 2021; Pidgeon et al. 2017; Wang et al. 2014). The phosphorus content (P ion is an important cation in charge balance with water) in metamict zircons is indeed lower than that of crystalline zircons (Yang et al. 2022), suggesting that the primary water signature is disturbed. Thus, thermal annealing of Sz2 zircon cannot retrieve its primary water content, which has been partly lost in its geological history. In that case, the primary water content obtained from hydrothermally altered zircon only represents the minimum estimate of its original value (Fig. 9a). In addition, the thermal annealing method is no longer applicable to the case that hydrogen and oxygen isotope exchange occurred intensively between secondary water and zircon. However, intensive oxygen isotope exchange is uncommon for the extremely slow oxygen diffusion rate in zircon (Cherniak and Watson 2003).

$\delta^{18}O$ remains unchanged at 600 °C, >4 h, which implies the loss of secondary water does not cause oxygen isotopic fractionations between secondary water and zircon. As shown in Figure 9b, higher annealing temperature corresponds to a narrower $\delta^{18}O$ range. Proportion of low-$\delta^{18}O$ zircons (<4.7‰) has dropped from ~21% at <600 °C for 2 h to ~9% at >700 °C. Therefore, heating metamict zircons above 700 °C for a long time can yield more accurate oxygen isotope compositions. The distorted zircon crystal lattice has been fully restored under such high temperature, and the

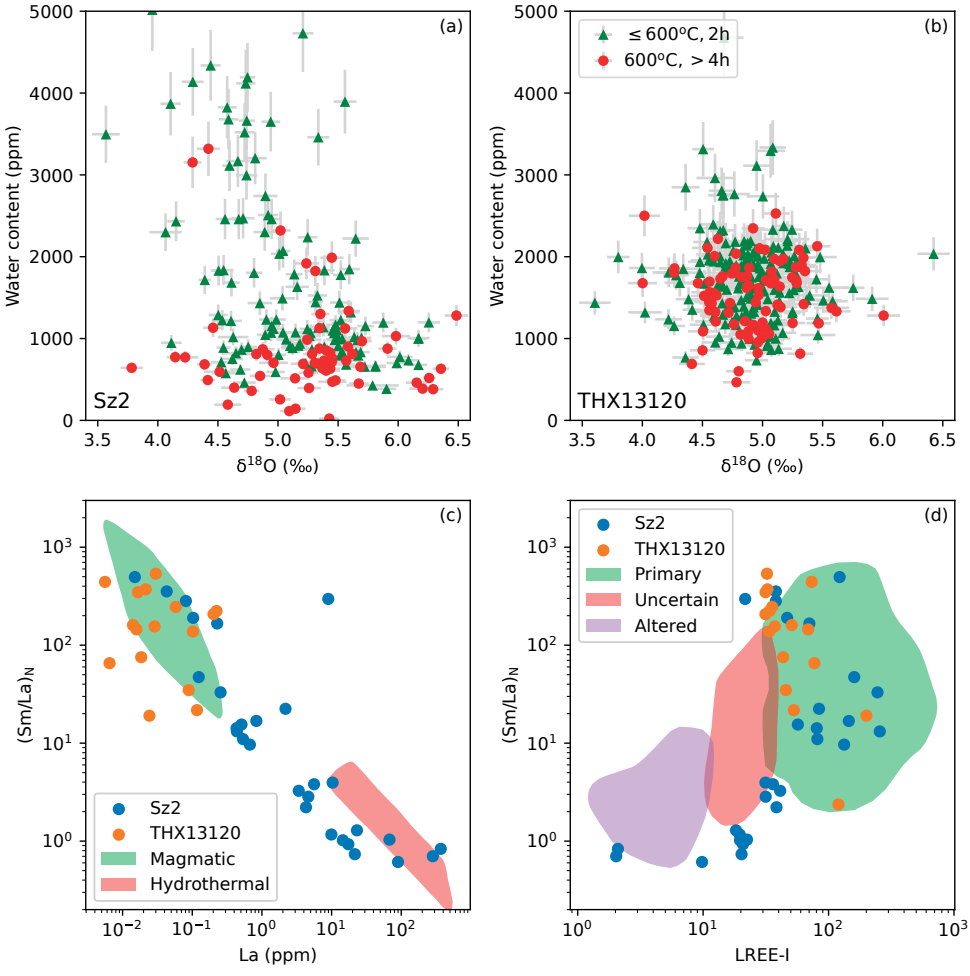

Figure 7. Plots of water content vs. $\delta^{18}O$ of Sz2 (**a**) and THX13120 (**b**). The zircons unannealed or annealed at <600 °C for 2 h are denoted by green triangles. They preserved their secondary waters from thermal diffusion. The zircon grains that were annealed at 600 °C for >4 h are marked with red circles, in which the secondary water was effectively removed. Error bars indicate 2σ errors; (**c**–**d**) discrimination plots of magmatic and hydrothermal zircons. $(Sm/La)_N$ is chondrite-normalized (Hoskin 2005), while LREE-I (LREE index) is defined by (Dy/Nd)+(Dy/Sm) (Bell et al. 2016).

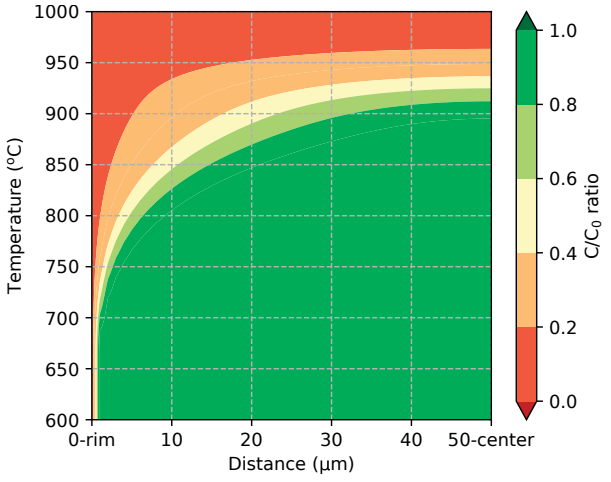

Figure 8. Calculated ratio of annealed zircon water content to its initial water content, according to Xu et al. (2019). The zircons with 100 μm diameter are assumed to be heated at 600–1000 °C for 2 h (see text for details).

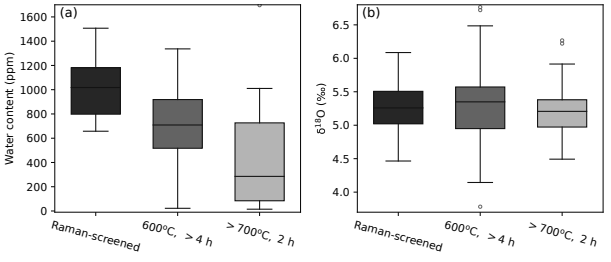

Figure 9. Water content (**a**) and $\delta^{18}O$ (**b**) of three zircon groups from Sz2. The Raman-screened crystalline zircons preserve primary geochemical signature. The zircons annealed at 600 °C for >4 h likely retrieve the primary water contents but expel all secondary water. By contrast, heating at >700 °C for 2 h likely removed both primary and secondary waters.

matrix effect (e.g., on zircon U-Pb isotope analysis) is effectively suppressed (Fig. 6) (Allen and Campbell 2012), accompanied by dramatic decreases in both primary and secondary water contents (Fig. 9a). The more accurate $\delta^{18}O$ measurement of zircons annealed at >700 °C likely resulted from the elimination of fractionation of secondary water and matrix effect from the metamict zircons.

Implications

From our annealing experiments (200–1000 °C for 2 h and 600 °C for 2–10 h), the following conclusions can be drawn:

(1) Heating at 600 °C for >4 h appears to be the optimal treatment condition for obtaining primary water content from metamict zircons.

(2) Hydrothermally altered zircons may have lost some of their primary water during metamictization. Consequently, thermal annealing of these zircons can only yield the minimum estimate of their primary water content.

(3) Thermal annealing at >700 °C could improve the oxygen isotope measurement by eliminating secondary water and matrix effect from metamict zircons.

(4) Thermal annealing of zircon has great potential in recovering primary water and oxygen isotope contents from metamict zircons, especially for those from geologically ancient samples.

Funding

This study was supported by the National Natural Science Foundation of China (41673010, 41688130), the Key Special Project for Introduced Talents Team of Southern Marine Science and Engineering Guangdong Laboratory (Guangzhou) (GML2019ZD0202) and the Strategic Priority Research Program of the Chinese Academy of Sciences (XDB18000000). We thank Li Ao for helping with the Raman spectroscopic analyses. This is contribution no. IS-3154. from GIGCAS.

References cited

Aines, R.D. and Rossman, G.R. (1986) Relationships between radiation-damage and trace water in zircon, quartz, and topaz. American Mineralogist, 71, 1186–1193.

Allen, C.M. and Campbell, I.H. (2012) Identification and elimination of a matrix-induced systematic error in LA-ICP-MS $^{206}Pb/^{238}U$ dating of zircon. Chemical Geology, 332–333, 157–165, https://doi.org/10.1016/j.chemgeo.2012.09.038.

Bell, E.A., Boehnke, P., and Harrison, T.M. (2016) Recovering the primary geochemistry of Jack Hills zircons through quantitative estimates of chemical alteration. Geochimica et Cosmochimica Acta, 191, 187–202, https://doi.org/10.1016/j.gca.2016.07.016.

Caruba, R., Baumer, A., Ganteaume, M., and Iacconi, P. (1985) An experimental-study of hydroxyl-groups and water in synthetic and natural zircons—A model of the metamict state. American Mineralogist, 70, 1224–1231.

Chakoumakos, B.C., Murakami, T., Lumpkin, G.R., and Ewing, R.C. (1987) Alpha-decay—induced fracturing in zircon: The transition from the crystalline to the metamict state. Science, 236, 1556–1559, https://doi.org/10.1126/science.236.4808.1556.

Cherniak, D.J. and Watson, E.B. (2003) Diffusion in zircon. Reviews in Mineralogy and Geochemistry, 53, 113–143, https://doi.org/10.2113/0530113.

Cui, Z.-X., Xia, X.-P., Huang, X.-L., Xu, J., Yang, Q., Zhang, W.-F., Zhang, L., Lai, C.-K., and Wang, X. (2022) Meso- to Neoarchean geodynamic transition of the North China Craton indicated by H_2O-in-zircon for TTG suite. Precambrian Research, 371, 106574, https://doi.org/10.1016/j.precamres.2022.106574.

De Hoog, J.C.M., Lissenberg, C.J., Brooker, R.A., Hinton, R., Trail, D., and Hellebrand, E., and EIMF. (2014) Hydrogen incorporation and charge balance in natural zircon. Geochimica et Cosmochimica Acta, 141, 472–486, https://doi.org/10.1016/j.gca.2014.06.033.

Diwu, C., Sun, Y., Zhao, Y., and Lai, S. (2014) Early Paleoproterozoic (2.45–2.20 Ga) magmatic activity during the period of global magmatic shutdown: Implications for the crustal evolution of the southern North China Craton. Precambrian Research, 255, 627–640, https://doi.org/10.1016/j.precamres.2014.08.001.

Ewing, R.C., Meldrum, A., Wang, L.M., Weber, W.J., and Corrales, L.R. (2003) Radiation effects in zircon. Reviews in Mineralogy and Geochemistry, 53, 387–425, https://doi.org/10.2113/0530387.

Gao, Y.Y., Li, X.H., Griffin, W.L., O'Reilly, S.Y., and Wang, Y.F. (2014) Screening criteria for reliable U-Pb geochronology and oxygen isotope analysis in uranium-rich zircons: A case study from the Suzhou A-type granites, SE China. Lithos, 192-195, 180–191, https://doi.org/10.1016/j.lithos.2014.02.002.

Hoskin, P.W.O. (2005) Trace-element composition of hydrothermal zircon and the alteration of Hadean zircon from the Jack Hills, Australia. Geochimica et Cosmochimica Acta, 69, 637–648, https://doi.org/10.1016/j.gca.2004.07.006.

Hoskin, P.W.O. and Schaltegger, U. (2003) The composition of zircon and igneous and metamophic petragenesis. Reviews in Mineralogy and Geochemistry, 53, 27–62, https://doi.org/10.2113/0530027.

Huang, C., Wang, H., Yang, J.H., Ramezani, J., Yang, C., Zhang, S.B., Yang, Y.H., Xia, X.P., Feng, L.J., Lin, J., and others. (2019) SA01—A proposed zircon reference material for microbeam U-Pb age and Hf-O Isotopic determination. geostandards and geoanalytical research, 44, 103–123, https://doi.org/10.1111/ggr.12307.

Ingrin, J. and Zhang, P.P. (2016) Hydrogen diffusion in zircon. EGU General Assembly Conference Abstracts, 18, EPSC2016–7148, Vienna.

Kemp, A.I., Hawkesworth, C.J., Foster, G.L., Paterson, B.A., Woodhead, J.D., Hergt, J.M., Gray, C.M., and Whitehouse, M.J. (2007) Magmatic and crustal differentiation history of granitic rocks from Hf-O isotopes in zircon. Science, 315, 980–983, https://doi.org/10.1126/science.1136154.

Li, X.H., Long, W.G., Li, Q.L., Liu, Y., Zheng, Y.F., Yang, Y.H., Chamberlain, K.R., Wan, D.F., Guo, C.H., Wang, X.C., and others. (2010) Penglai zircon megacrysts: A potential new working reference material for microbeam determination of Hf-O isotopes and U-Pb age. Geostandards and Geoanalytical Research, 34, 117–134, https://doi.org/10.1111/j.1751-908X.2010.00036.x.

Li, X.H., Tang, G.Q., Gong, B., Yang, Y.H., Hou, K.J., Hu, Z.C., Li, Q.L., Liu, Y., and Li, W.X. (2013) Qinghu zircon: A working reference for microbeam analysis of U-Pb age and Hf and O isotopes. Chinese Science Bulletin, 58, 4647–4654, https://doi.org/10.1007/s11434-013-5932-x.

Liebmann, J., Spencer, C.J., Kirkland, C.L., Xia, X.P., and Bourdet, J. (2021) Effect of water on $\delta^{18}O$ in zircon. Chemical Geology, 574, 120243, https://doi.org/10.1016/j.chemgeo.2021.120243.

Lu, J.S., Zhai, M.G., Lu, L.S., Wang, H.Y.C., Chen, H.X., Peng, T., Wu, C.M., and Zhao, T.P. (2017) Metamorphic *P-T-t* path retrieved from metapelites in the southeastern Taihua metamorphic complex, and the Paleoproterozoic tectonic evolution of the southern North China Craton. Journal of Asian Earth Sciences, 134, 352–364, https://doi.org/10.1016/j.jseaes.2016.12.001.

Meng, J.T., Xia, X.P., Ma, L., Jiang, Z.Q., Xu, J., Cui, Z.X., Yang, Q., Zhang, W.F., and Zhang, L. (2021) A H_2O-in-zircon perspective on the heterogeneous water content of crust-derived magmas in southern Tibet. Science China. Earth Sciences, 64, 1184–1194, https://doi.org/10.1007/s11430-020-9790-1.

Nasdala, L., Irmer, G., and Wolf, D. (1995) The degree of metamictization in zircon: A Raman-spectroscopic study. European Journal of Mineralogy, 7, 471–478, https://doi.org/10.1127/ejm/7/3/0471.

Nasdala, L., Pidgeon, R.T., and Wolf, D. (1996) Heterogeneous metamictization of zircon on a microscale. Geochimica et Cosmochimica Acta, 60, 1091–1097, https://doi.org/10.1016/0016-7037(95)00454-8.

Nasdala, L., Beran, A., Libowitzky, E., and Wolf, D. (2001a) The incorporation of hydroxyl groups and molecular water in natural zircon ($ZrSiO_4$). American Journal of Science, 301, 831–857, https://doi.org/10.2475/ajs.301.10.831.

Nasdala, L., Wenzel, M., Vavra, G., Irmer, G., Wenzel, T., and Kober, B. (2001b) Metamictisation of natural zircon: Accumulation versus thermal annealing of radioactivity-induced damage. Contributions to Mineralogy and Petrology, 141, 125–144, https://doi.org/10.1007/s004100000235.

Nasdala, L., Zhang, M., Kempe, U., Panczer, G., Gaft, M., Andrut, M., and Plotze, M. (2003) Spectroscopic methods applied to zircon. Reviews in Mineralogy and Geochemistry, 53, 427–467, https://doi.org/10.2113/0530427.

Palenik, C.S., Nasdala, L., and Ewing, R.C. (2003) Radiation damage in zircon. American Mineralogist, 88, 770–781, https://doi.org/10.2138/am-2003-5606.

Pidgeon, R.T. (2014) Zircon radiation damage ages. Chemical Geology, 367, 13–22, https://doi.org/10.1016/j.chemgeo.2013.12.010.

Pidgeon, R.T., Nemchin, A.A., and Cliff, J. (2013) Interaction of weathering solutions with oxygen and U-Pb isotopic systems of radiation-damaged zircon from an Archean granite, Darling Range Batholith, Western Australia. Contributions to Mineralogy and Petrology, 166, 511–523, https://doi.org/10.1007/s00410-013-0888-z.

Pidgeon, R.T., Nemchin, A.A., and Whitehouse, M.J. (2017) The effect of weathering on U-Th-Pb and oxygen isotope systems of ancient zircons from the Jack Hills, Western Australia. Geochimica et Cosmochimica Acta, 197, 142–166, https://doi.org/10.1016/j.gca.2016.10.005.

Schmidt, C. and Nasdala, L. (2020) Applications of Raman spectroscopy in mineralogy and geochemistry. Elements (Quebec), 16, 99–104, https://doi.org/10.2138/gselements.16.2.99.

Trail, D., Thomas, J.B., and Watson, E.B. (2011) The incorporation of hydroxyl into zircon. American Mineralogist, 96, 60–67, https://doi.org/10.2138/am.2011.3506.

Valley, J.W., Chiarenzelli, J.R., and McLelland, J.M. (1994) Oxygen isotope geochemistry of zircon. Earth and Planetary Science Letters, 126, 187–206, https://doi.org/10.1016/0012-821X(94)90106-6.

Wang, X.L., Coble, M.A., Valley, J.W., Shu, X.J., Kitajima, K., Spicuzza, M.J., and Sun, T. (2014) Influence of radiation damage on Late Jurassic zircon from southern China: Evidence from in situ measurements of oxygen isotopes, laser Raman, U-Pb ages, and trace elements. Chemical Geology, 389, 122–136, https://doi.org/10.1016/j.chemgeo.2014.09.013.

Wang, R., Jeon, H., and Evans, N.J. (2018) Archaean hydrothermal fluid modified zircons at Sunrise Dam and Kanowna Belle gold deposits, Western Australia: Implications for post-magmatic fluid activity and ore genesis. American Mineralogist, 103, 1891–1905, https://doi.org/10.2138/am-2018-6402.

White, L.T. and Ireland, T.R. (2012) High-uranium matrix effect in zircon and its implications for SHRIMP U-Pb age determinations. Chemical Geology, 306–307, 78–91, https://doi.org/10.1016/j.chemgeo.2012.02.025.

Woodhead, J.A., Rossman, G.R., and Silver, L.T. (1991a) The metamictization of zircon: Radiation dose-dependent structural characteristics. American Mineralogist, 76, 74–82.

Woodhead, J.A., Rossman, G.R., and Thomas, A.P. (1991b) Hydrous species in zircon. American Mineralogist, 76, 1533–1546.

Xia, X.P., Cui, Z.X., Li, W.C., Zhang, W.F., Yang, Q., Hui, H.J., and Lai, C.K. (2019) Zircon water content: Reference material development and simultaneous measurement of oxygen isotopes by SIMS. Journal of Analytical Atomic Spectrometry, 34, 1088–1097, https://doi.org/10.1039/C9JA00073A.

Xia, X.P., Meng, J.T., Ma, L., Spencer, C.J., Cui, Z.X., Zhang, W.F., Yang, Q., and Zhang, L. (2021) Tracing magma water evolution by H_2O-in-zircon: A case study in the Gangdese batholith in Tibet. Lithos, 404-405, 106445, https://doi.org/10.1016/j.lithos.2021.106445.

Xu, Y., Tang, W., Hui, H., Rudnick, R.L., Shang, S., and Zhang, Z. (2019) Reconciling the discrepancy between the dehydration rates in mantle olivine and pyroxene during xenolith emplacement. Geochimica et Cosmochimica Acta, 267, 179–195, https://doi.org/10.1016/j.gca.2019.09.023.

Xu, J., Xia, X.P., Wang, Q., Spencer, C.J., Lai, C.K., Ma, J.L., Zhang, L., Cui, Z.X., Zhang, W.F., and Zhang, Y.Q. (2021) Pure sediment-derived granites in a subduction zone. Geological Society of America Bulletin, 134, 599–615, https://doi.org/10.1130/B36016.1.

Yang, C.M., Xu, Y.G., Xiao, X.P., Gao, Y.Y., Zhang, W.F., Yang, Y.N., Yang, Q., and Zhang, L. (2022) Raman spectroscopy-based screening of zircon for reliable water content and oxygen isotope measurements. American Mineralogist, 107, 936–945, https://doi.org/10.2138/am-2022-8075.

Yao, J., Cawood, P.A., Zhao, G., Han, Y., Xia, X., Liu, Q., and Wang, P. (2021) Mariana-type ophiolites constrain the establishment of modern plate tectonic regime during Gondwana assembly. Nature Communications, 12, 4189, https://doi.org/10.1038/s41467-021-24422-z.

Zhai, M.G., Guo, J.H., and Liu, W.J. (2005) Neoarchean to Paleoproterozoic continental evolution and tectonic history of the North China Craton: A review. Journal of Asian Earth Sciences, 24, 547–561, https://doi.org/10.1016/j.jseaes.2004.01.018.

Zhang, P.P. (2015) Hydrogen diffusion in NAMs: andradite garnet and zircon. Unité Matériaux et Transformations, Doctor, 218. Université de Lille.

Zhang, M., Salje, E.K.H., and Ewing, R.C. (2003) Oxidation state of uranium in metamict and annealed zircon: Near-infrared spectroscopic quantitative analysis. Journal of Physics: Condensed Matter, 15, 3445–3470, https://doi.org/10.1088/0953-8984/15/20/307.

——— (2010) OH species, U ions, and CO/CO_2 in thermally annealed metamict zircon ($ZrSiO_4$). American Mineralogist, 95, 1717–1724, https://doi.org/10.2138/am.2010.3567.

Zhang, W.F., Xia, X.P., Zhang, Y.Q., Peng, T.P., and Yang, Q. (2018) A novel sample preparation method for ultra-high vacuum (UHV) secondary ion mass spectrometry (SIMS) analysis. Journal of Analytical Atomic Spectrometry, 33, 1559–1563, https://doi.org/10.1039/c8ja00087e.

Manuscript received January 5, 2022
Manuscript accepted March 10, 2022
Accepted manuscript online March 23, 2022
Manuscript handled by Fang-Zhen Teng

Endnote:

[1]Deposit item AM-23-38444, Online Materials. Deposit items are free to all readers and found on the MSA website, via the specific issue's Table of Contents (go to http://www.minsocam.org/MSA/AmMin/TOC/2023/Mar2023_data/Mar2023_data.html).